

Statefinder diagnosis and the interacting ghost model of dark energy

M. Malekjani¹ *, A. Khodam-Mohammadi^{†1}

¹*Department of Physics, Faculty of Science,
Bu-Ali Sina University, Hamedan 65178, Iran*

Abstract

A new model of dark energy namely "ghost dark energy model" has recently been suggested to interpret the positive acceleration of cosmic expansion. The energy density of ghost dark energy is proportional to the hubble parameter. In this paper we perform the statefinder diagnostic tool for this model both in flat and non-flat universe. We discuss the dependency of the evolutionary trajectories in $s - r$ and $q - r$ planes on the interaction parameter between dark matter and dark energy as well as the spatial curvature parameter of the universe. Eventually, in the light of SNe+BAO+OHD+CMB observational data, we plot the evolutionary trajectories in $s - r$ and $q - r$ planes for the best fit values of the cosmological parameters and compare the interacting ghost model with other dynamical dark energy models. We show that the evolutionary trajectory of ghost dark energy in statefinder diagram is similar to holographic dark energy model. It has been shown that the statefinder location of Λ CDM is in good agreement with observation and therefore the dark energy models whose current statefinder values are far from the Λ CDM point can be ruled out.

* Email: malekjani@basu.ac.ir

† Email: khodam@basu.ac.ir

I. INTRODUCTION

Nowadays it is strongly believed that our universe expands under an accelerated expansion. The various cosmological data gathered from SNe Ia [1], WMAP [2], SDSS [3] and X-ray [4] experiments have provided the main evidences for this cosmic acceleration. Within the framework of standard cosmology, a dark energy component with negative pressure is responsible for this acceleration. Up to now many theoretical models have been proposed to interpret the behavior of dark energy. The first and simple candidate is the Einstein's cosmological constant with the time - independent equation of state $w_\Lambda = -1$. The cosmological constant suffers from tow deep theoretical problems namely the "fine-tuning" and "cosmic coincidence". In addition to cosmological constant, dynamical dark energy model with time-varying equation of state have been investigated to interpret the cosmic acceleration. The scalar field models such as quintessence [5], phantom [6], quintom [7], K-essence [8], tachyon [9] and dilaton [10] together with interacting dark energy models such as holographic [11] and agegraphic [12] models are the examples of dynamical dark energy models. The interacting dark energy models have been constructed within the framework of quantum gravity, by introducing the new degree of freedom or by modifying the theory of gravity [13–15]. Recently, the Veneziano ghost dark energy has been attracted a deal of attention in the dynamical DE category. The Veneziano ghost is proposed to solve the $U(1)$ problem in low-energy effective theory of QCD [16] and has no contribution in the flat Minkowski spacetime. In curved spacetime, however, it makes a small energy density proportional to $\Lambda_{QCD}^3 H$, where Λ_{QCD} is QCD mass scale and H is Hubble parameter. This small vacuum energy density can be considered as a driver engine for evolution of the universe. It is worthwhile to mention that this model is totally arisen from standard model and general relativity. Therefore one needs not to introduce any new parameter or new degree of freedom and this fact is the most advantages of ghost DE. With $\Lambda_{QCD} \sim 100 Mev$ and $H \sim 10^{-33} ev$, the right order of observed DE density can be given by ghost DE. This numerical coincidence also shows that this model gets ride of fine tuning problem [17, 18] Many authors have already suggested DE model with energy density as $\rho = \alpha H$ [19].

Recent observational data gathered from the Abell Cluster A586 support the interaction between dark matter and dark energy [20]. However the strength of this interaction is not clearly identified [21].

Since many theoretical dark energy models have been proposed to explain the accelerated expansion of the universe, therefore the sensitive test which can differentiate between these models is required. The Hubble parameter, $H = \dot{a}/a$, (first time derivative) and the deceleration parameter $q = -\ddot{a}H^2/a$ (second time derivative) are the geometrical parameters to describe the expansion history of the universe. $\dot{a} > 0$ or $H > 0$ means the expansion of the universe. Also $\ddot{a} > 0$, i.e. $q < 0$, indicates the accelerated expansion of the universe. Since the various dark energy models give $H > 0$, $q < 0$ at the present time, the Hubble and deceleration parameters can not discriminate dark energy models. For this aim we need a higher order of time derivative of scale factor. Sahni et al. [22] and Alam et al. [23], by using the third time derivative of scale factor, introduced the statefinder pair $\{s, r\}$ in order to remove the degeneracy of H and q at the present time. The statefinder pair is given by

$$r = \frac{\ddot{a}}{aH^3}, s = \frac{r-1}{3(q-1/2)} \quad (1)$$

Depending the statefinder diagnostic tool on the scale factor indicates that the statefinder parameters are geometrical. The scale factor $a(t)$ can be expanded near the present time t_0 as follows

$$a(t) = 1 + H_0(t - t_0) - \frac{1}{2}q_0H_0^2(t - t_0)^2 + \frac{1}{6}r_0H_0^3(t - t_0)^3 + \dots \quad (2)$$

where we consider $a(t_0) = 1$ and H_0 , q_0 , r_0 are the present values of the Hubble parameter, deceleration parameter and former statefinder parameter, respectively. Up to now, the various dark energy models have been studied from the viewpoint of statefinder diagnostic. These models have different evolutionary trajectories in $\{s, r\}$ plane, therefore the statefinder tool can discriminate these models. The well known Λ CDM model is related to the fixed point $\{s=0, r=1\}$ in the $s-r$ plane [22]. The distance of the current value of statefinder pair $\{s_0, r_0\}$ for a given dark energy model from the fixed point $\{s=0, r=1\}$ is a valuable criterion to a model. In addition, the distance of current statefinder values of a given dark energy model from the constrained observational value $\{s_0, r_0\}$ is a good tool to test a model.

The dynamical dark energy models that have been investigated by statefinder diagnostic tool are:

the quintessence DE model [22, 23], the interacting quintessence models [24, 25], the holographic dark energy models [26, 27], the holographic dark energy model in non-flat universe [28], the phantom model [29], the tachyon [30], the generalized chaplygin gas model [31], the interacting new agegraphic DE model in flat and non-flat universe [32, 33], the agegraphic

dark energy model with and without interaction in flat and non-flat universe [34, 35], the new holographic dark energy model [36] and the interacting polytropic gas model [39].

In this work we investigate the interacting ghost dark energy model by statefinder diagnostic tool. The statefinder can be applied to diagnose different cases of the model, including different model parameters and different contributions of spatial curvature. First, we perform the statefinder diagnostic in flat universe in sect. II, then we generalize our work to the non flat universe in sect. III. In sect.IV, the statefinder diagnostic has been discussed based on recent observational data. This work is concluded in sect. V.

II. INTERACTING GHOST DARK ENERGY MODEL IN FLAT UNIVERSE

Let us first consider the interacting ghost dark energy in the flat Friedmann-Robertson-Walker (FRW) universe. The corresponding Friedmann equation in this case is given by

$$H^2 = \frac{1}{3M_p^2}(\rho_m + \rho_\Lambda) \quad (3)$$

where H and M_p are the Hubble parameter and the reduced Planck mass, respectively. The energy density of ghost dark energy is given by [50]

$$\rho_\Lambda = \alpha H \quad (4)$$

where α is a constant of the model. The dimensionless energy densities are defined as

$$\Omega_m = \frac{\rho_m}{\rho_c} = \frac{\rho_m}{3M_p^2 H^2}, \quad \Omega_\Lambda = \frac{\rho_\Lambda}{\rho_c} = \frac{\rho_\Lambda}{3M_p^2 H^2} \quad (5)$$

Using (5), the Friedmann equation (3) can be written as

$$\Omega_m + \Omega_\Lambda = 1. \quad (6)$$

In a universe dominated by interacting dark energy and dark matter, the total energy density, $\rho = \rho_m + \rho_\Lambda$, satisfies the following conservation equation

$$\dot{\rho} + 3H(\rho + p) = 0 \quad (7)$$

However, by considering the interaction between dark energy and dark matter, the energy density of dark energy and dark matter does not conserve separately and the conservation

equation for each component is given by

$$\dot{\rho}_m + 3H\rho_m = Q, \quad (8)$$

$$\dot{\rho}_\Lambda + 3H(\rho_\Lambda + p_\Lambda) = -Q, \quad (9)$$

where Q represents the interaction between dark matter and dark energy. It is worth noting that in equation (8) the right hand side of (8), same as left hand side, should be as a function of inverse of time. The simple choice is that the interaction quantity Q can be considered as a function of Hubble parameter H such as one of the following forms: (i) $Q \propto H\rho_\Lambda$, (ii) $Q \propto H\rho_m$ and (iii) $Q \propto H(\rho_m + \rho_\Lambda)$. One can assume the above three forms as $Q = \Gamma\rho_\Lambda$, where for case (i) $\Gamma = 3b^2H$, for case (ii) $\Gamma = 3b^2H\frac{\Omega_m}{\Omega_\Lambda}$ and for case (iii) $\Gamma = 3b^2H\frac{1}{\Omega_\Lambda}$. The parameter b is a coupling constant indicating the strength of interaction between dark matter and dark energy [52]. The interaction between dark energy and dark matter is also studied in [53]. Here we assume the third form of interaction for Q .

Taking the time derivative from both side of Friedmann equation (3) and using (6, 8, 9) as well as the relation $p_\Lambda = w_\Lambda\rho_\Lambda$, one can obtain

$$\frac{\dot{H}}{H^2} = -\frac{3}{2}[1 + w_\Lambda\Omega_\Lambda] \quad (10)$$

Inserting the third form of interaction term $Q = \Gamma\rho_\Lambda = 3b^2H\frac{1}{\Omega_\Lambda}\rho_\Lambda$ in the right hand side of (9) and using the relations (4), (10), the equation of state for interacting ghost dark energy in the flat universe can be obtained as

$$w_\Lambda = \frac{-1}{2 - \Omega_\Lambda}\left(1 + \frac{2b^2}{\Omega_\Lambda}\right) \quad (11)$$

In the limiting case of non-interacting flat universe (i.e., $b = 0$ and $\Omega_k = 0$), Eq.(11) reduces to

$$w_\Lambda = -\frac{1}{2 - \Omega_\Lambda} \quad (12)$$

which is in agreement with [51]. At the early time when $\Omega_\Lambda \ll 1$, we can see $w_\Lambda = -1/2$ and at the late time when $\Omega_\Lambda \sim 1$, one can see $w_\Lambda = -1$. Therefore the ghost dark energy mimics the cosmological constant at the late time. The evolution of EoS parameter of ghost model has been studied in [51]. It has been shown that the interacting ghost dark energy model can cross the phantom divide for $b^2 > 0.1$.

Using (10), the deceleration parameter q in this model can be obtained as

$$q = -1 - \frac{\dot{H}}{H^2} = \frac{1}{2} + \frac{3}{2}w_\Lambda\Omega_\Lambda \quad (13)$$

It is clear that at the early time (when $\Omega_\Lambda \rightarrow 0$) we have $q = 1/2$ which is equal to the value of deceleration parameter obtained in CDM model. Therefore in ghost model, the decelerated expansion phase ($q > 0$) at the early time can be achieved. At the late time (when $\Omega_\Lambda \sim 1$ and $w_\Lambda = -1$), we see that $q = -1$, which represents the accelerated expansion ($q < 0$) in dark energy dominated universe, as expected.

Tacking the time derivative of dark energy density parameter in (5) and using the ghost dark energy density (4), we have

$$\dot{\Omega}_\Lambda = -\frac{\alpha \dot{H}}{3M_p^2 H^2} \quad (14)$$

Using (13) and $\dot{\Omega}_\Lambda = H\Omega'_\Lambda$ yields

$$\Omega'_\Lambda = \frac{3}{2}\Omega_\Lambda(1 + w_\Lambda\Omega_\Lambda) \quad (15)$$

where prime denotes the derivative with respect to $\ln a$. Tacking the time derivative of (10) and using (5), (9) and (4) we obtain

$$\frac{\ddot{H}}{H^3} = \frac{9}{4}w_\Lambda\Omega_\Lambda(w_\Lambda\Omega_\Lambda + 3) - \frac{3}{2}\Omega_\Lambda w'_\Lambda + \frac{18}{4} \quad (16)$$

We now find the statefinder parameters $\{s, r\}$ for the interacting ghost dark energy model in the flat universe. From the definition of q and H , the parameter r in (1) can be written as

$$r = \frac{\ddot{H}}{H^3} - 3q - 2. \quad (17)$$

Substituting the relations (13) and (16) in (17), the parameter r is obtained as

$$r = 1 + \frac{9}{4}w_\Lambda\Omega_\Lambda(w_\Lambda\Omega_\Lambda + 1) - \frac{3}{2}\Omega_\Lambda w'_\Lambda \quad (18)$$

Inserting Eqs. (13) and (18) in the parameter s of (1) obtains

$$s = \frac{1}{2}(1 + w_\Lambda\Omega_\Lambda) - \frac{w'_\Lambda}{3w_\Lambda} \quad (19)$$

At the late time (when $\Omega_\Lambda \rightarrow 1$), by inserting $w_\Lambda = -1$ and therefore $w'_\Lambda = 0$, the relations (18) and (19) reduce to the constant values ($r = 1$, $s = 0$) which refers the statefinder parameters of standard Λ CDM model in the flat universe. Therefore, from the viewpoint of statefinder diagnostic, the ghost dark energy mimics the cosmological constant at the late time.

By numerical solving of Eqs. (18) and (19), we obtain the evolutionary trajectory of interacting ghost dark energy in the statefinder plane. It should be noted that in Eqs. (18) and (19) the evolution of w_Λ and Ω_Λ are governed by Eqs. (15) and (11), respectively. In statefinder plane, the horizontal axis is defined by the parameter s and vertical axis by the parameter r . In this diagram, the standard Λ CDM model corresponds to the fixed point $\{r = 1, s = 0\}$.

In Fig.(1), we plot the evolutionary trajectories of ghost dark energy model in the flat universe in $s - r$ plane for different illustrative values of interaction parameter b . Here we adopt the current values of cosmological parameters Ω_Λ and Ω_m as 0.7 and 0.3, respectively. The standard Λ CDM fixed point $\{r = 1, s = 0\}$ is indicated by star symbol in this diagram. The colored circles on the curves show the present values of statefinder pair $\{s_0, r_0\}$. By expanding the universe, the trajectories in $s - r$ plane start from right to left. The parameter r decreases, then increases to the constant value $r = 1$ at the late time. While the parameter s decreases from the positive value at the early time to the constant value $s = 0$ at the late time. Different values of interaction parameter b result the different evolutionary trajectories in $s - r$ plane. Hence the statefinder analysis can discriminate the interacting ghost dark energy model with different interaction parameter. For larger value of b , the present values of s_0 and r_0 decreases. The distance of the point $\{s_0, r_0\}$ from the Λ CDM fixed point $\{s = 0, r = 1\}$ becomes larger for larger values of interaction parameter b . Fig.(1) also shows that the interacting ghost dark energy model mimics the Λ CDM model at the late time. This behavior of ghost dark energy is similar to the holographic [26–28], new agegraphic [32, 33], chaplygin gas [37], generalized chaplygin gas [31] and yang-mills [38] models of dark energy in which they also mimic the Λ CDM model at the late time.

Unlike the above models, the agegraphic dark energy model [34, 35] and polytropic gas model [39] mimic the Λ CDM model at the early stage of the evolution of the universe. The evolutionary trajectories of holographic dark energy under granda-Oliveros IR cut-off (new holographic model) [36] and also tachyon dark energy model [30] in $s - r$ plane pass through the Λ CDM fixed point at the middle of the evolution of the universe. The other interesting note is that the evolution of ghost dark energy model in $s - r$ plane is similar to the evolution of holographic model of dark energy with the model parameter $c = 1$ in this plane (i.e., see Fig.(3) of [27] and upper panel of Fig.(1) in [28]).

Also, it is of interest to discuss the dynamical behavior of ghost dark energy in $q - r$ plane.

In $q-r$ plane, we use the geometrical quantity q instead of the parameter s at the horizontal axis. In Fig.(2), by solving Eqs.(13) and (18), the evolutionary trajectories of ghost dark energy in flat universe is plotted for different values of interaction parameter b in $q-r$ plane. Same as statefinder analysis, the $q-r$ analysis can discriminate different dark energy models. By expanding the universe, the trajectories start from right to left. The parameter r decrease, then increases to the constant value $r = 1$ at the late time. While the parameter q decreases from the positive value (indicating the decelerated expansion) at the early time to the negative value (representing the accelerated expansion) at the late time. Here we see the different evolutionary trajectories for different interaction parameters b . The current value $\{q_0, r_0\}$ can also be affected by interaction parameter. Increasing the interaction parameter b causes both the parameters r and q becomes smaller.

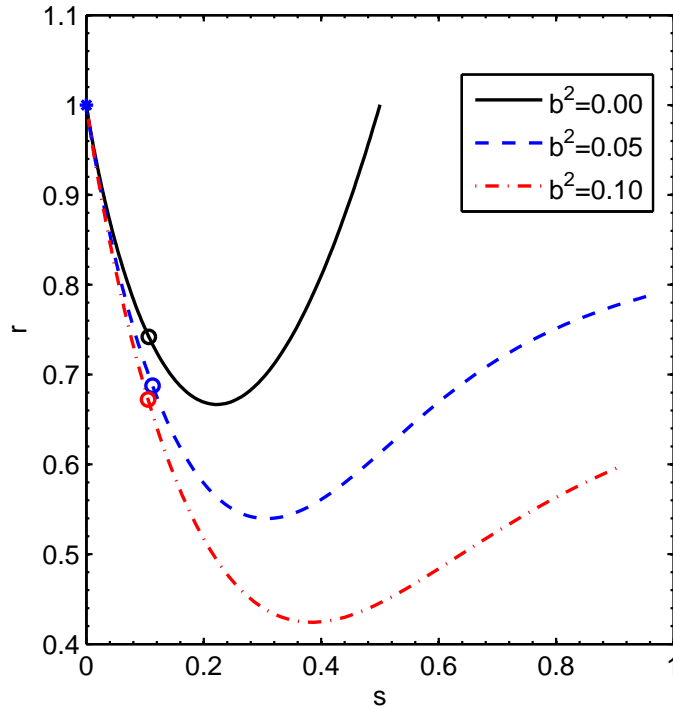


FIG. 1: The evolutionary trajectories in $s-r$ plane for interacting ghost dark energy model in the flat universe with the cosmological parameters $\Omega_{m0} = 0.3$ and $\Omega_{\Lambda 0} = 0.7$. The location of standard Λ CDM fixed point is indicated by star symbol. The colored circle points are the location of present values of statefinder pair $\{s_0, r_0\}$ for different interaction parameter as described in legend.

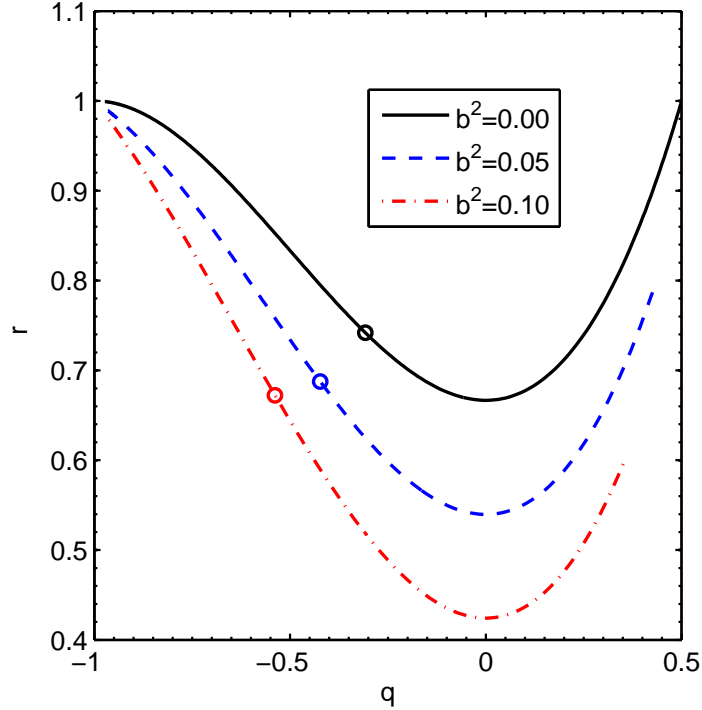


FIG. 2: The evolutionary trajectories in $q-r$ plane for interacting ghost dark energy model in the flat universe with the cosmological parameters $\Omega_{m0} = 0.3$ and $\Omega_{\Lambda 0} = 0.7$. The colored circle points are the location of present values of statefinder pair $\{q_0, r_0\}$ for different interaction parameter as described in legend.

III. INTERACTING GHOST DARK ENERGY MODEL IN A NON FLAT UNIVERSE

In this section we generalize our work in previous section to the non flat universe. The Friedmann equation in this case is given by

$$H^2 + \frac{k}{a^2} = \frac{1}{3M_p^2}(\rho_m + \rho_\Lambda) \quad (20)$$

where $k = 1, 0, -1$ is a spatial curvature parameter corresponding to the closed, flat and open universe, respectively. The dimensionless energy densities of dark energy and dark matter have been defined in (5) and dimensionless energy density corresponding to the spatial curvature is given as $\Omega_k = \frac{k}{a^2 H^2}$. Therefore the Friedmann equation (20) in terms of dimensionless parameters is written as

$$\Omega_m + \Omega_\Lambda = 1 + \Omega_k. \quad (21)$$

Same as previous section, here in the non flat universe, we consider the third form of interaction between dark matter and dark energy $Q \propto H(\rho_m + \rho_\Lambda)$. Using Eqs. (20) and (21), this form of interaction in non flat universe can be written as $Q = \Gamma \rho_\Lambda$, where $\Gamma = 3b^2 H \frac{1+\Omega_k}{\Omega_\Lambda}$. Taking the time derivative of both side of Friedmann equation (20) and using (21, 8, 9) as well as the relation $p_\Lambda = w_\Lambda \rho_\Lambda$, one can obtain

$$\frac{\dot{H}}{H^2} = \Omega_k - \frac{3}{2}[1 + \Omega_k + w_\Lambda \Omega_\Lambda] \quad (22)$$

where Ω_k is given by

$$\Omega_k = \frac{a\gamma(1 - \Omega_\Lambda)}{1 - a\gamma}, \quad \gamma = \frac{\Omega_{k0}}{\Omega_{m0}} \quad (23)$$

Inserting the interaction term Q in the right hand side of continuity equation (9) and using the relations (4), (22), the equation of state for interacting ghost dark energy in the non flat universe can be obtained as

$$w_\Lambda = \frac{2}{2 - \Omega_\Lambda} \left[-1 + \frac{1}{2}(1 + \Omega_k) \left(1 - \frac{2b^2}{\Omega_\Lambda}\right) - \frac{\Omega_k}{3} \right] \quad (24)$$

In the limiting case of flat universe (i.e., $\Omega_k = 0$), Eq.(24) reduces to (11), as expected. Using (22), the deceleration parameter q in non flat case can be obtained as

$$q = -1 - \frac{\dot{H}}{H^2} = \frac{1}{2}(1 + \Omega_k) + \frac{3}{2}w_\Lambda \Omega_\Lambda \quad (25)$$

The evolution of dark energy density in non flat universe is obtained by tacking the time derivative of (5) and using the ghost dark energy density (4)

$$\dot{\Omega}_\Lambda = -\frac{\alpha \dot{H}}{3M_p^2 H^2} \quad (26)$$

Using (25) and $\dot{\Omega}_\Lambda = H\Omega'_\Lambda$ results

$$\Omega'_\Lambda = \Omega_\Lambda(1 + q) \quad (27)$$

where q is defined in (25). Tacking the time derivative of Eq. (22) and using (5), (9), (23) and (24) results

$$\frac{\ddot{H}}{H^3} = \frac{9}{4}w_\Lambda\Omega_\Lambda(w_\Lambda\Omega_\Lambda + 3) - \frac{3}{2}\Omega_\Lambda(w'_\Lambda - \Omega_k w_\Lambda \frac{\Omega_\Lambda - 3/2}{\Omega_\Lambda - 1}) + \Omega_k \frac{\Omega_\Lambda(\Omega_k + 7) - 10}{4(\Omega_\Lambda - 1)} + \frac{18}{4} \quad (28)$$

Inserting Eqs. (25) and (28) in Eq. (17), the former statefinder parameter r for interacting ghost dark energy in the non flat universe is obtained as

$$r = 1 + \frac{9}{4}w_\Lambda\Omega_\Lambda(w_\Lambda\Omega_\Lambda + 1) - \frac{3}{2}\Omega_\Lambda(w'_\Lambda - \Omega_k w_\Lambda \frac{\Omega_\Lambda - 3/2}{\Omega_\Lambda - 1}) + \Omega_k \frac{\Omega_\Lambda(1 + \Omega_k) - 4}{4(\Omega_\Lambda - 1)} \quad (29)$$

Following [55], we consider the parameter s in the non flat universe as follows

$$s = \frac{r - \Omega_t}{3(q - \Omega_t/2)} \quad (30)$$

where $\Omega_t = 1 + \Omega_k$ is a total energy density as defined in Friedmann equation. Obviously, in the limiting case of flat universe, i.e., $\Omega_k = 0$, the above definition is reduced to (1).

Substituting Eqs. (25) and (29) in (30) gets

$$s = \frac{1}{2}(1 + w_\Lambda\Omega_\Lambda) - \frac{w'_\Lambda}{3w_\Lambda} + \frac{\Omega_k}{3(\Omega_\Lambda - 1)} \left(\Omega_\Lambda - 3/2 + \frac{\Omega_k - 3}{6w_\Lambda} \right) \quad (31)$$

In the limiting case of flat universe, the above equations for the statefinder parameter $\{s, r\}$ are reduced to those obtained in previous section. Here in this section, we focus on the contribution of spatial curvature on the evolution of ghost dark energy in the $s - r$ and $q - r$ planes. For this aim we need to solve numerically the relations (25, 29 and 31). Note that in these equations the dynamics of EoS parameter w_Λ , density parameter Ω_Λ and spatial curvature parameter Ω_k are given by (24), (5) and (23), respectively.

In Fig.(3), we plot the statefinder diagram for different contribution of spatial curvatures. The selected curves are plotted by fixing $\Omega_{m0} = 0.30$, $\Omega_{\Lambda0} = 0.70$ and varying $\Omega_{k0} = 0.02$, $\Omega_{k0} = 0.00$ and $\Omega_{k0} = -0.02$ corresponding to the closed, flat and open universe, respectively. A closed universe with a small positive curvature ($\Omega_k = 0.02$) is compatible with some observations [56]. Here we ignore the interaction between dark matter and dark energy and focus only on the effect of contribution of spatial curvature on the evolution of trajectories in statefinder plane. By expanding the universe, the trajectories evolve from right to left. The parameter r decreases, then increases and reaches to the constant value $r = 1$ at the late time. The parameter s decreases forever. The different contributions of spatial curvature exhibit the different features in the $s - r$ plane. The colored circles on the curves are the today's

value of $\{s_0, r_0\}$ for different spatial curvatures. One can see that the today's value $\{s_0, r_0\}$ of interacting ghost dark energy with different spatial curvatures is discriminated. We can clearly identify the distance from a given dark energy model to the standard flat- Λ CDM model by using the $r(s)$ evolution diagram. Fig.(3) shows that in the closed universe the distance of the present value $\{s_0, r_0\}$ from the location of Λ CDM fixed point $\{s = 0, r = 1\}$ is shorter compare with other spatial curvatures. The holographic dark energy model from the viewpoint of statefinder diagnostic analysis in the non flat universe has already been investigated in [28]. By comparing Fig.(3) with upper panel of Fig.(1) of [28], we see the similarity of evolutionary trajectories between ghost dark energy model and the holographic model of dark energy (with the model parameter $c = 1$) in non flat universe.

Fig.(4) shows the evolutionary trajectories of interacting ghost dark energy in $q-r$ plane for different contributions of spatial curvature of the universe. By expanding the universe the trajectories evolve from right to left, the parameter r first decreases then increases and the parameter q decreases from the positive value at the early time (indicating the decelerated phase of expansion) to the negative value at the at late time (denoting the accelerated phase). In $q-r$ plane, the interacting ghost model is discriminated for different contribution of spatial curvatures. The current value of statefinder pair $\{q_0, r_0\}$ is also distinguished in different spatial curvatures of the universe. The value of $\{q_0, r_0\}$ is larger in closed universe ($\Omega_k = 0.02$) compare with flat ($\Omega_k = 0.00$) and open ($\Omega_k = -0.02$) universe.

IV. INTERACTING GHOST MODEL AND OBSERVATIONAL CONSTRAINS

It is clear that constraining the parameterized model against the observational data is model dependent. Hence some doubts usually remain on the validity of the constraints on the derived quantities such as the present day values of the deceleration parameter and the age of the universe. In order to solve this problem, we use the cosmography, i.e. the expansion of scale factor in Taylor series with respect to the cosmic time. For this aim, the

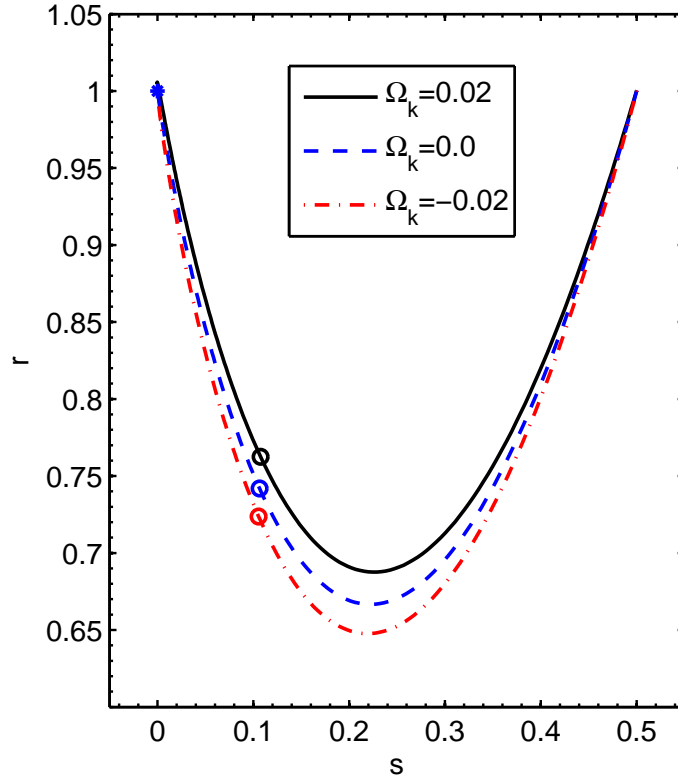


FIG. 3: The evolutionary trajectories of ghost dark energy model in $s - r$ plane for different contributions of spatial curvatures $\Omega_{k0} = 0.02$ (closed universe), $\Omega_{k0} = 0.00$ (flat universe), $\Omega_{k0} = -0.02$ (open universe). Here we set $\Omega_{m0} = 0.3$ and $\Omega_{\Lambda 0} = 0.7$. The colored circle points are the location of present value $\{s_0, r_0\}$ for different spatial curvature as indicated in legend. The location of Λ CDM fixed point has been shown by star symbol.

following functions

$$H = \frac{1}{a} \frac{da}{dt} \quad (32)$$

$$q = -\frac{1}{a} \frac{d^2 a}{dt^2} H^{-2} \quad (33)$$

$$r = \frac{1}{a} \frac{d^3 a}{dt^3} H^{-3} \quad (34)$$

$$k = \frac{1}{a} \frac{d^4 a}{dt^4} H^{-4} \quad (35)$$

$$l = \frac{1}{a} \frac{d^5 a}{dt^5} H^{-5} \quad (36)$$

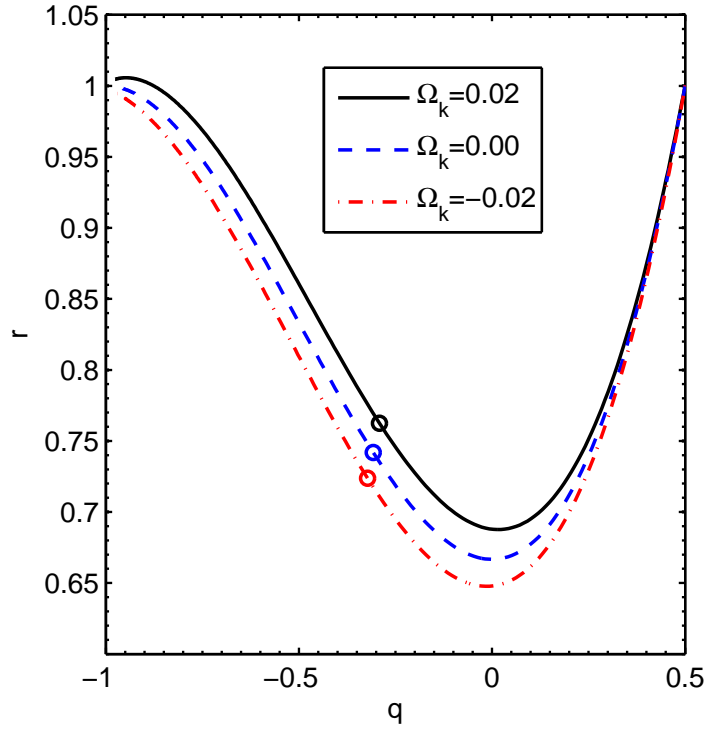


FIG. 4: The evolutionary trajectories of ghost dark energy model in $q - r$ plane for different contributions of spatial curvatures $\Omega_{k0} = 0.02$ (closed universe), $\Omega_{k0} = 0.00$ (flat universe), $\Omega_{k0} = -0.02$ (open universe). Here we set $\Omega_{m0} = 0.3$ and $\Omega_{\Lambda 0} = 0.7$. The colored circle points are the location of present value $\{q_0, r_0\}$ for different spatial curvature as indicated in legend.

which are namely the Hubble, deceleration, jerk, snap and lerk parameters, respectively are introduced. The present values of the above parameters can be used to describe the evolution of the universe. For example, $q_0 < 0$ indicates the current accelerated expansion of the universe and also r_0 allows to discriminate between different dark energy models. Using the Union2 SNeIa data set [59] and the BAO data from the analysis of the SDSS seventh release [60] adding a prior on h from the recent determination of the Hubble constant by the SHOES team [61] and the age of passively evolving galaxies [58], the present values of the above cosmographic parameters are constrained observationally by using the Markov Chain Monte Carlo method [57]. The best fit values of the cosmographic parameters are: $\{h = 0.718, q_0 = -0.64, r_0 = 1.02, k_0 = -0.39, l_0 = 4.05\}$ (see table I of [57] for more details).

Inserting the present values of $q_0 = -0.64$ and $r_0 = 1.02$ in Eq. (1), the present value of statefinder parameter s is obtained as $s_0 = -0.006$. Therefore, observationally, the best fit value of the current statefinder pair is $\{s_0 = -0.006, r_0 = 1.02\}$. In this section we compare the present value of statefinder parameters $\{s, r\}$ of interacting ghost dark energy that has been constrained observationally in [51] with the above best fit value of current statefinder pair.

For this aim we use the best fit constrained values of the cosmological parameters $\Omega_{m0} = 0.35$, $\Omega_{\Lambda 0} = 0.75$ and $b^2 = 0.08$ in the ghost dark energy model that have recently been obtained in [51] by using the data of Supernova type Ia (SNIa) Gold sample, shift parameter of Cosmic Microwave Background radiation (CMB) and the Baryonic Acoustic Oscillation (BAO) peak from Sloan Digital Sky Survey (SDSS). In Fig.(5) the evolutionary trajectories of interacting ghost dark energy in $s - r$ plane (upper panel) and in $q - r$ plane (lower panel) are plotted for the above best fit values of cosmological parameters Ω_{m0} , $\Omega_{\Lambda 0}$ and b^2 . In $s - r$ diagram, the evolutionary trajectory starts from $\{s = 0.86, r = 0.67\}$ at the past time, reaches to the $\{s = 0.08, r = 0.74\}$ at the present time (circle point) and ended at $\{s = 0, r = 1\}$ at the future. The best fit observational value $\{s_0 = -0.006, r_0 = 1.02\}$ in flat universe is indicated by red-star symbol in this diagram. In $q - r$ diagram, the evolutionary trajectory starts from $\{q = 0.4, r = 1\}$ at the past (corresponds to the decelerated expansion of the universe), reaches to $\{q = -0.6, r = 0.74\}$ at the present time and ended at $\{q = -1, r = 1\}$ at the late time (corresponds to the accelerated expansion). The best fit observational value $\{q_0 = -0.64, r_0 = 1.02\}$ is also indicated by red-star symbol in this diagram.

Now we compare the present value $\{s_0, r_0\}$ of constrained interacting ghost dark energy model with other models of dark energy which have been constrained and discussed from the viewpoint of statefinder diagnostic. This comparison includes the interacting ghost model, holographic, new holographic and generalized chaplygin gas models of dark energy. These models have been constrained by astronomical data of SNe+CMB+BAO+OHD experiments and also have been discussed in $s - r$ diagram based on the constrained values of cosmological and model parameters. This comparison also includes the standard Λ CDM model as well as the best fit observational value $\{s_0 = -0.006, r_0 = 1.02\}$ in flat universe. The holographic dark energy model with the constrained values ($c = 0.84$, $\Omega_{m0} = 0.29$, $\Omega_{k0} = 0.02$, where c is the model parameter of holographic dark energy) obtains the today's statefinder pair as $\{s_0 = -0.102, r_0 = 1.357\}$ [28]. The new holographic dark energy model with the

constrained values ($\Omega_b h^2 = 0.0228$, $\Omega_{m0} = 0.2762$, $\Omega_{k0} = 0.0305$, $\Omega_{\Lambda 0} = 0.6934$, $\alpha = 0.8824$, $\beta = 0.5016$, where α and β are the parameters of model) results the today's statefinder pair as $\{s_0 = -0.13, r_0 = 1.46\}$ [36]. The generalized chaplygin gas dark energy (GCG model) in the flat universe with the constrained values ($A_s = 0.76$, $\alpha = 0.033$, $\Omega_b h^2 = 0.0233$, $H_0 = 69.97$, where A_s and α are the parameters of the model) gives the today's statefinder pair as $\{s_0 = -0.007, r_0 = 1.026\}$ [31]. Note that the GCG model is constrained in the flat universe, but other models are constrained in general non-flat universe. Fig.(6) shows the location of the present statefinder pair $\{s_0, r_0\}$ for the above constrained models as indicated in legend. The standard Λ CDM model and also the best fit observational value $\{s_0 = -0.006, r_0 = 1.02\}$ in flat universe are indicated by black and red star symbols, respectively. One can conclude that the Λ CDM model $\{s = 0, r = 1\}$ has a shortest distance to the best fit observational value $\{s_0 = -0.006, r_0 = 1.02\}$ compare to other dynamical dark energy models. Also, the interacting ghost dark energy model has a shorter distance from $\{s_0 = -0.006, r_0 = 1.02\}$ compare with the holographic and new holographic dark energy models. Among the dynamical dark energy model, the GCG model has a shortest distance from the location of observational value in $s - r$ plane.

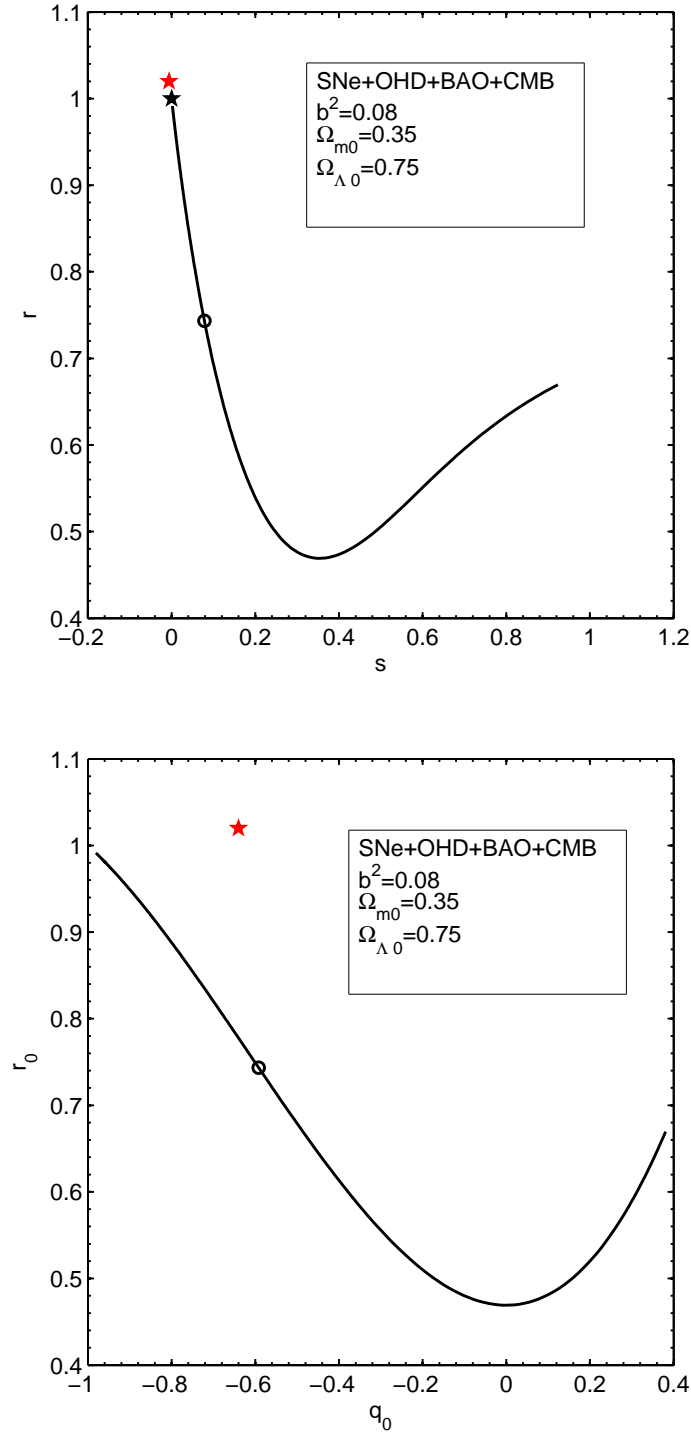


FIG. 5: The statefinder diagrams $r(s)$ (upper panel) and $r(q)$ (lower panel) for interacting ghost dark energy model. The evolutionary trajectories are plotted in the light of best fit result of SNe + OHD + BAO + CMB, $\Omega_{\Lambda 0} = 0.75$, $\Omega_{m0} = 0.35$ and $b^2 = 0.08$. The circle points on the curves show the today's value $\{s_0, r_0\}$, upper panel, and $\{q_0, r_0\}$, lower panel. For comparison, the standard Λ CDM model has been shown by black-star symbol and the constrained observational value of $\{s_0, r_0\}$ and $\{q_0, r_0\}$ are indicated by red-star symbol in these diagrams.

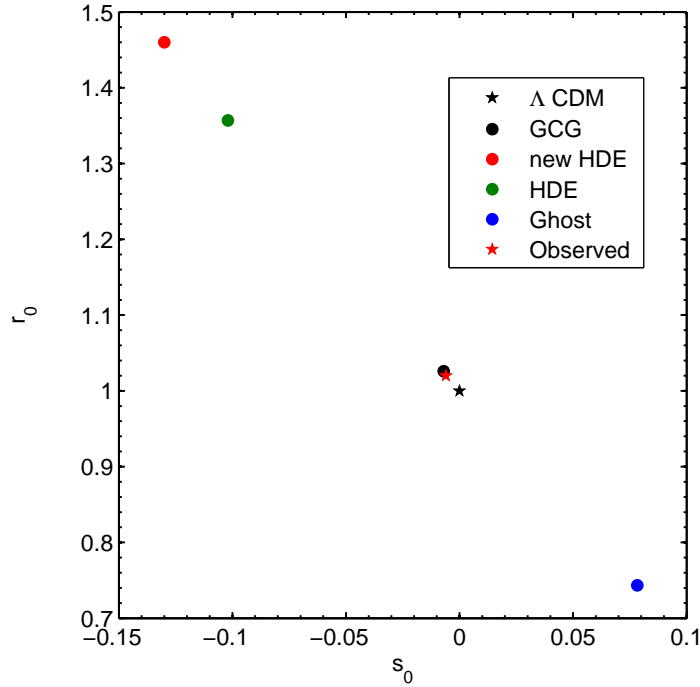


FIG. 6: The present value of $\{s_0, r_0\}$ in the light of best fit result of SNe + OHD + BAO + CMB observations for different dark energy model as indicated in legend. The location of standard Λ CDM model and constrained observational value $\{s_0, r_0\}$ have been shown by black and red star symbols, respectively.

V. CONCLUSION

Summarizing this work, we investigated the interacting ghost dark energy model in statefinder $s - r$ and $q - r$ diagrams. The statefinder analysis can discriminate the interacting ghost dark energy model for different values of interaction parameter as well as the different spatial curvatures of the universe. Like holographic [26–28], new agegraphic [32, 33], chaplygin gas [37], generalized chaplygin gas [31] and yang-mils [38] models of dark energy, the ghost dark energy model mimics the standard Λ CDM model at the late time. The evolution of ghost dark energy model in $s - r$ plane is similar to holographic model of dark energy with the model parameter $c = 1$. Different values of interaction parameter obtains the different evolutionary trajectories in $s - r$ and $q - r$ planes. The evolutionary trajectories $r(s)$ and $r(q)$ for interacting ghost dark energy model in different closed, flat

and open universe has also been investigated. We have shown that different contribution of spatial curvatures give the different evolutionary trajectories in $s - r$ and $q - r$. The spatial curvature can also influence the present value of statefinder parameters $\{s_0, r_0\}$ and $\{q_0, r_0\}$ in these planes. Eventually, we performed the statefinder diagnostic for the interacting ghost model constrained by observational data. We conclude that the Λ CDM model $\{s = 0, r = 1\}$ has a shortest distance to the best fit observational value $\{s_0 = -0.006, r_0 = 1.02\}$ compare with other dynamical dark energy models. Therefore the models of dark energy whose current statefinder values locate far from the Λ CDM point can be ruled out. The interacting ghost dark energy model has a shorter distance from $\{s_0 = -0.006, r_0 = 1.02\}$ compare with the holographic and new holographic dark energy models. Among the above dynamical dark energy models, the GCG model has a shortest distance from the location of observational statefinder pair (i.e., $\{s_0 = -0.006, r_0 = 1.02\}$).

-
- [1] S. Perlmutter et al., *Astrophys. J.* **517**, 565 (1999).
 - [2] C. L. Bennett et al., *Astrophys. J. Suppl.* **148**, 1 (2003).
 - [3] M. Tegmark et al., *Phys. Rev. D* **69**, 103501 (2004).
 - [4] S. W. Allen, et al., *Mon. Not. Roy. Astron. Soc.* **353**, 457 (2004).
 - [5] C. Wetterich, *Nucl. Phys. B* **302**, 668 (1988);
B. Ratra, J. Peebles, *Phys. Rev. D* **37**, 321 (1988).
 - [6] R. R. Caldwell, *Phys. Lett. B* **545**, 23 (2002);
S. Nojiri, S.D. Odintsov, *Phys. Lett. B* **562**, 147 (2003);
S. Nojiri, S.D. Odintsov, *Phys. Lett. B* **565**, 1 (2003).
 - [7] E. Elizalde, S. Nojiri, S.D. Odinstov, *Phys. Rev. D* **70**, 043539 (2004);
S. Nojiri, S.D. Odintsov, S. Tsujikawa, *Phys. Rev. D* **71**, 063004 (2005);
A. Anisimov, E. Babichev, A. Vikman, *J. Cosmol. Astropart. Phys.* **06**, 006 (2005).
 - [8] T. Chiba, T. Okabe, M. Yamaguchi, *Phys. Rev. D* **62**, 023511(2000);
C. Armendariz-Picon, V. Mukhanov, P.J. Steinhardt, *Phys. Rev. Lett.* **85**, 4438 (2000);
C. Armendariz-Picon, V. Mukhanov, P.J. Steinhardt, *Phys. Rev. D* **63**, 103510 (2001).
 - [9] A. Sen, *J. High Energy Phys.* **04**, 048 (2002);
T. Padmanabhan, *Phys. Rev. D* **66**, 021301 (2002);

- T. Padmanabhan, T.R. Choudhury, Phys. Rev. D **66**, 081301 (2002).
- [10] M. Gasperini, F. Piazza, G. Veneziano, Phys. Rev. D **65**, 023508 (2002);
 N. Arkani-Hamed, P. Creminelli, S. Mukohyama, M. Zaldarriaga, J. Cosmol. Astropart. Phys. **04**, 001 (2004);
 F. Piazza, S. Tsujikawa, J. Cosmol. Astropart. Phys. **07**, 004 (2004).
- [11] P. Horava, D. Minic, Phys. Rev. Lett. **85**, 1610 (2000);
 P. Horava, D. Minic, Phys. Rev. Lett. **509**, 138 (2001);
 S. Thomas, Phys. Rev. Lett. **89**, 081301 (2002);
 M. R. Setare, Phys. Lett. B **644**, 99, 2007;
 M. R. Setare, Phys. Lett. B **654**, 1, 2007;
 M. R. Setare, Phys. Lett. B **642**, 1, 2006;
 M. R. Setare, Eur. Phys. J. C **50**, 991, 2007;
 M. R. Setare, Phys. Lett. B **648**, 329, 2007;
 M. R. Setare, Phys. Lett. B **653**, 116, 2007.
- [12] R.G. Cai, Phys. Lett. B **657**, (2007) 228;
 H. Wei, R.G. Cai, Phys. Lett. B **660**, 113 (2008).
- [13] G. 't Hooft, gr-qc/9310026;
 L. Susskind, J. Math. Phys. **36**, 6377 (1995).
- [14] F. Karolyhazy, Nuovo.Cim. A **42** (1966) 390;
 F. Karolyhazy, A. Frenkel and B. Lukacs, in Physics as natural Philosophy edited by A. Shimony and H. Feshbach, MIT Press, Cambridge, MA, (1982);
 F. Karolyhazy, A. Frenkel and B. Lukacs, in Quantum Concepts in Space and Time edited by R. Penrose and C.J. Isham, Clarendon Press, Oxford, (1986).
- [15] A. Sheykhi, Phys. Lett. B **680** (2009) 113;
 A. Sheykhi, Phys Lett B **681** (2009) 205;
 A. Sheykhi, Phys. Rev. D **81** (2010) 023525;
 A. Sheykhi, B. Wang and N. Riazi, Phys. Rev. D **75**, 123513 (2007).
- [16] E. Witten, Nucl. Phys. B **156**, 269 (1979);
 G. Veneziano, Nucl. Phys. B **159**, 213 (1979);
 C. Rosenzweig, j. Schechter and C. G. Trahern, Phys. Rev. D **21**, 3388 (1980);
 P. Nath and R. L. Arnowitt, Phys. Rev. D **23**, 473 (1981);

- K. Kawarabayashi and N. Ohta, Nucl. Phys. B **175**, 477 (1980);
 Prog. Theor. Phys. **66**, 1789 (1981);
 N. Ohta, Prog. Theor. Phys. **66**, 1408 (1981).
- [17] F. R. Urban and A. R. Zhitnitsky, Phys. Lett. B **688**, 9 (2010) (arXiv:0906.2162) [gr-qc]; Phys. Rev. D **80**, 063001 (2009) (arXiv:0906.2165) [hep-th]; JCAP **0909**, 018 (2009)(arXiv:0906.3546) [astro-ph.CO]; Nucl. Phys. B **835**, 135 (2010) (arXiv:0909.2684) [astro-ph.CO].
- [18] N. Ohta, Phys. Lett. B **695**, 41 (2011) 41.
- [19] J. Bjorken, arXiv:hep-th/0111196; R. Schutzhold, Phys. Rev. Lett. **89**, 081302 (2002);
 J. D. Bjorken, arXiv:astro-ph/0404233;
 F. R. Klinkhamer and G. E. Volovik, Phys. Rev. D **77**, 085015 (2008) [arXiv:0711.3170 [gr-qc]];
 F. R. Klinkhamer and G. E. Volovik, Phys. Rev. D **78**, 063528 (2008) [arXiv:0806.2805 [gr-qc]];
 F. R. Klinkhamer and G. E. Volovik, Phys. Rev. D **79**, 063527 (2009) [arXiv:0811.4347 [gr-qc]];
 Y. B. Zeldovich, JETP Lett. **6**, 316 (1967) [Pisma Zh. Eksp. Teor. Fiz. **6**, 883 (1967)];
 W. Zimdahl, H. A. Borges, S. Carneiro, J. C. Fabris and W. S. Hipolito-Ricardi, (arXiv:1009.0672) [astro-ph.CO];
 S. Nojiri and S. D. Odintsov, Phys. Rev. D **72**, 023003 (2005) [arXiv:hep-th/0505215];
 S. Capozziello, V. F. Cardone, E. Elizalde, S. Nojiri and S. D. Odintsov, Phys. Rev. D **73**, 043512 (2006) [arXiv:astro-ph/0508350].
- [20] O. Bertolami, F. Gil Pedro, M. Le Delliou, Phys. Lett. B **654**, 165 (2007).
- [21] C. Feng, B. Wang, Y. Gong, R.K. Su, JCAP **0709**, 005 (2007).
- [22] Sahni, V., Saini, T.D., Starobinsky, A.A., Alam, U.: JETP Lett. **77**, 201 (2003).
- [23] Alam, U., Sahni, V., Saini, T.D., Starobinsky, A.A.: Mon. Not. R. Astron. Soc. **344**, 1057 (2003b)
- [24] Zimdahl, W., Pavon, D.: Gen. Relativ. Gravit. **36**, 1483 (2004).
- [25] Zhang, X.: Phys. Lett. B **611**, 1 (2005a).
- [26] Zhang, X.: Int. J. Mod. Phys. D **14**, 1597 (2005b).
- [27] Zhang, J., Zhang, X., Liu, H.: arXiv:0705.4145 [astro-ph] (2007).

- [28] Setare, M.R., Zhang, J., Zhang, X.: J. Cosmol. Astropart. Phys. 0703, 007 (2007).
- [29] Chang, B.R., Liu, H.Y., Xu, L.X., Zhang, C.W., Ping, Y.L.: J. Cosmol. Astropart. Phys. 0701, 016 (2007).
- [30] Shao, Y., Gui, Y.: gr-qc/0703111.
- [31] Malekjani, M., Khodam-Mohammadi, A. and N. Nazari-Pooya, Astrophys Space Sci, 334:193201, 2011.
- [32] Zhang, L., Cui, J., Zhang, J., Zhang, X.: Int. J. Mod. Phys. D 19,21 (2010)
- [33] Khodam-Mohammadi, A., Malekjani, M.: Astrophys. Space Sci. 331, 265 (2010).
- [34] Wei, H., Cai, R.G.: Phys. Lett. B 655, 1 (2007)
- [35] Malekjani, M., Khodam-Mohammadi, A.: Int. J. Mod. Phys. D 19,1 (2010).
- [36] Malekjani, M., Khodam-Mohammadi, A., Nazari-Pooya, N., Astrophys Space Sci (2011) 332: 515524.
- [37] Gorini, V., Kamenshchik, A., Moschella, U., arxiv:astro-ph/0209395.
- [38] Zhao, W., arXiv:0711.2319.
- [39] Malekjani, M., Khodam-Mohammadi, A., M. Taji, arxiv:1201.—
- [40] Scherrer, R.J.: Phys. Rev. D 73, 043502 (2006)
- [41] Chiba, T.: Phys. Rev. D 73, 063501 (2006)
- [42] Barger, V., Guarnaccia, E., Marfatia, D.: Phys. Lett. B 635, 61 (2006)
- [43] Zhao, W.: Phys. Rev. D 73, 123509 (2006)
- [44] Zhao, W.: Phys. Lett. B 655, 97 (2007)
- [45] Calcagni, G., Liddle, A.R.: Phys. Rev. D 74, 043528 (2006)
- [46] Guo, Z.K., Piao, Y.S., Zhang, X.M., Zhang, Y.Z.: Phys. Rev. D 74, 127304 (2006)
- [47] Huang, Z.G., Li, X.H., Sun, Q.Q.: Astrophys. Space Sci. 310,53 (2007a)
- [48] Huang, Z.G., Lu, H.Q., Fang, W.: Int. J. Mod. Phys. D 16, 1109 (2007b)
- [49] de Putter, R., Linder, E.V.: Astropart. Phys. 28, 263 (2007)
- [50] N. Ohta, Phys. Lett. B 695 (2011) 41.
- [51] A. Sheykhi, M. Sadegh. Movahed, arXiv: 1104.4713.
- [52] A. Sheykhi, Phys. Lett. B **680**, 113 (2009); H. Wei & R. G. Cai, Phys. Lett. B **660**, 113 (2008); L. Zhang, J. Cui, J. Zhang & X. Zhang, Int. J. Mod. Phys. D **19**, 21 (2010).
- [53] L. P. Chimento, Phys. Rev. D **81**, 043525 (2010).
- [54] Malekjani. M., Khodam-Mohammadi. A., Nazari-Pooya, N., Astrophys Space Sci (2011) 332:

515524.

- [55] Evans, A.K.D., Wehus, I.K., Gron, O., Elgaroy, O.: *Astron. Astrophys.* 430, 399 (2005).
- [56] C. L. Bennett, et al., *Astrophys. J. Suppl.* 148 (2003) 1; D. N. Spergel, *Astrophys. J. Suppl.* 148 (2003) 175; M. Tegmark, et al., *Phys. Rev. D* 69 (2004) 103501; U. Seljak, A. Slosar, P. McDonald, *JCAP* 0610 (2006) 014; D. N. Spergel, et al., *Astrophys. J. Suppl.* 170 (2007) 377.
- [57] Capozziello, S., Cardone, V. F., Farajollahi, H., Ravanpak, A. [arXiv:1108.2789](https://arxiv.org/abs/1108.2789).
- [58] E. Gaztanaga, A. Cabre, L. Hui, *MNRAS*, 399, 1663, 2009.
- [59] R. Amanullah, C. Lidman, D. Rubin, G. Aldering, P. Astier et al., *ApJ*, 716, 712, 2010
- [60] W.J. Percival, B.A. Reid, D.J. Eisenstein, N.A. Bahcall, T. Budavari, et al., *MNRAS*, 401, 2148, 2010.
- [61] A.G. Riess, L. Macri, W. Li, H. Lampeitl, S. Casertano et al., *ApJ* 699, 539, 2009